

Kinetic Characteristics of FCC to Hexagonal Transformation in $(\text{Ge}_1\text{Sb}_2\text{Te}_4)_{0.8}(\text{Sn}_1\text{Bi}_2\text{Te}_4)_{0.2}$ Chalcogenide Alloy for Phase Change Memory

Dong-Ho Ahn, Hyun-Mi Kim, Min-Hyun Lee,
Dae-Hwan Kang¹, Byung-ki Cheong¹, and Ki-Bum Kim*

School of Materials Science and Engineering, Seoul National University, Seoul 151-742, Korea
¹Thin Film Materials Research Center, Korea Institute of Science and Technology, Seoul 136-791, Korea

We examined the kinetic characteristics of the fcc to hexagonal transformation in a $(\text{Ge}_1\text{Sb}_2\text{Te}_4)_{0.8}(\text{Sn}_1\text{Bi}_2\text{Te}_4)_{0.2}$ chalcogenide alloy mixture, which was utilized to propose a phase change memory in our recent study. Our examination involved *in-situ* measurement of temperature-dependent sheet resistance along with transmission electron microscopy (TEM) analysis. The $(\text{Ge}_1\text{Sb}_2\text{Te}_4)_{0.8}(\text{Sn}_1\text{Bi}_2\text{Te}_4)_{0.2}$ alloy was found to transform from an as-deposited *fcc* crystalline phase to an *hcp* crystalline phase at 485 K; by contrast, $\text{Ge}_1\text{Sb}_2\text{Te}_4$ transformed from an as-deposited *amorphous* phase to an *fcc* crystalline phase at 370 K. By use of Kissinger's method, we determined the activation energies of the transformations respectively as 1.85 eV for $\text{Ge}_1\text{Sb}_2\text{Te}_4$ and 2.98 eV for $(\text{Ge}_1\text{Sb}_2\text{Te}_4)_{0.8}(\text{Sn}_1\text{Bi}_2\text{Te}_4)_{0.2}$. The activation energy of 2.98 eV for $(\text{Ge}_1\text{Sb}_2\text{Te}_4)_{0.8}(\text{Sn}_1\text{Bi}_2\text{Te}_4)_{0.2}$ was found to be lower than that of the *fcc* to *hcp* phase transformation of $\text{Ge}_2\text{Sb}_2\text{Te}_5$. We consider that such a lower activation energy is partly responsible for a rapid *fcc* to *hcp* transition in the phase-change memory with $(\text{Ge}_1\text{Sb}_2\text{Te}_4)_{0.8}(\text{Sn}_1\text{Bi}_2\text{Te}_4)_{0.2}$ as a memory material.

Keywords: amorphous semiconductor, chalcogenide, phase transformation, nonvolatile memory, phase-change memory (PCM), Kissinger's method

1. INTRODUCTION

Phase-change random access memory (PCRAM) is a promising candidate for next-generation nonvolatile memory devices because of its many advantages, including nonvolatility, process simplicity, and high scalability. However, some critical problems with PCRAM must be overcome before it can be mass produced; these problems include a high operation current, thermal interference between cells, and low data retention property. These obstacles tend to have origins closely related to the temperatures of phase changes of a memory material: a high operation current is related to a high melting temperature, while a low retention and thermal interference are related to a low crystallization (transition) temperature. In a conventional phase-change memory with a GeSbTe stoichiometry compound, data are stored in forms of electrical resistance difference between an amorphous phase and a crystalline *fcc* phase. Additionally, the reversible transition behavior of PCRAM is attained by the crystallization and melt-quenching process between the *amorphous* and *fcc* phases^[1]. In a previous study, we reported on a newly designed phase change memory using $(\text{Ge}_1\text{Sb}_2\text{Te}_4)_{0.8}(\text{Sn}_1\text{Bi}_2\text{Te}_4)_{0.2}$ that

reversibly changes from *fcc* to *hcp*, or vice versa, during a short pulse duration of 70 ns^[2]. This new memory device utilizes phase change material having the ideal properties of a higher transition temperature and a lower melting temperature, both of which are the result of the addition of $\text{Sn}_1\text{Bi}_2\text{Te}_4$ into the $\text{Ge}_1\text{Sb}_2\text{Te}_4$ alloy.

In this study, we report on the phase transformation kinetics of the $(\text{Ge}_1\text{Sb}_2\text{Te}_4)_{0.8}(\text{Sn}_1\text{Bi}_2\text{Te}_4)_{0.2}$ alloy mixture, which we examined using the *in-situ* temperature dependence sheet resistance measurement and transmission electron microscopy (TEM) analysis. The aim of this work is to understand the origin of the fast data writing and good retention time of the newly designed PCRAM with $(\text{Ge}_1\text{Sb}_2\text{Te}_4)_{0.8}(\text{Sn}_1\text{Bi}_2\text{Te}_4)_{0.2}$ alloy.

2. EXPERIMENT

$\text{Ge}_1\text{Sb}_2\text{Te}_4$ and $(\text{Ge}_1\text{Sb}_2\text{Te}_4)_{0.8}(\text{Sn}_1\text{Bi}_2\text{Te}_4)_{0.2}$ films, each 100-nm thick, were deposited on the SiO_2/Si substrate via RF sputtering from an alloy target. The sheet resistances of the films were measured on the thermo chuck (Temptronic 03215b) with a four-point probe following a procedure proposed by van der Pauw^[3]. A sample was heated from room temperature to 300 °C at a controlled rate during each mea-

*Corresponding author: kikum@sun.ac.kr

surement. The temperature difference between a given sample and the heating chuck was compensated by a NiCr-Ni thermocouple in direct contact with the sample. Before and after the resistance transition, the microstructure and the structural phase of the samples were analyzed using the TEM micrographs and electron beam diffraction patterns.

3. RESULTS AND DISCUSSION

3.1. Temperature dependence of sheet resistance

Figure 1 shows a typical sheet resistance variance corresponding to the heating temperature in a case with a heating rate of 0.05 K/sec. Since $\text{Ge}_1\text{Sb}_2\text{Te}_4$ and $(\text{Ge}_1\text{Sb}_2\text{Te}_4)_{0.8}(\text{Sn}_1\text{Bi}_2\text{Te}_4)_{0.2}$ films are basically semiconductors, both sheet resistances are decreased as the temperature is increased by enhanced carrier concentration. Resistance slopes represent the activation energy for the conduction of the thermally activated carrier and an abrupt slope at a certain temperature region represents the resistance variation for the transition volume. In this study, we were not concerned with the conduction behavior or the transition volume change. Slopes before and after the transitions of both materials were similar, except for the gentle slope of $(\text{Ge}_1\text{Sb}_2\text{Te}_4)_{0.8}(\text{Sn}_1\text{Bi}_2\text{Te}_4)_{0.2}$ after 500 K. I. Friedrich *et al.* have been reported that this region is caused by a change of electronic structure in the *hcp* structure^[4]. Meanwhile, the sheet resistance values and the transition temperatures of the alloys were quite different. The origin of the differing transition temperature is a direct result of the different microstructures between these two films. The details of these structural differences will be discussed in the next section.

3.2. Micro structure and phase analysis

In the case of $\text{Ge}_1\text{Sb}_2\text{Te}_4$ alloy, sheet resistance is decreased

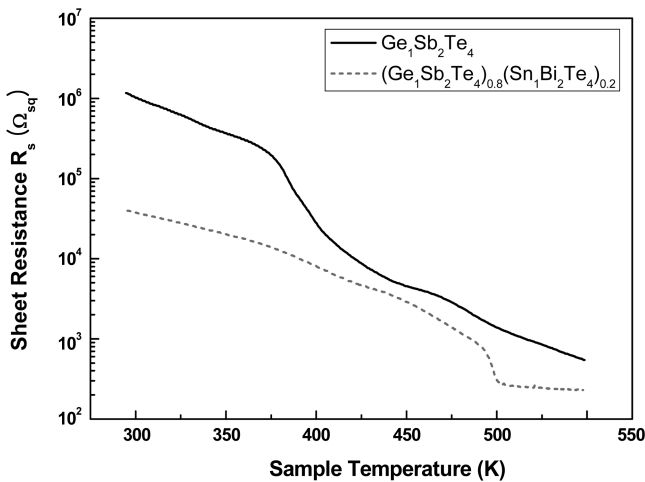


Fig. 1. Temperature dependent sheet resistance of $\text{Ge}_1\text{Sb}_2\text{Te}_4$ and $(\text{Ge}_1\text{Sb}_2\text{Te}_4)_{0.8}(\text{Sn}_1\text{Bi}_2\text{Te}_4)_{0.2}$. Data were measured in a 100-nm-thick film at heating rate of 0.05 K/sec.

as the heating temperature is increased, before it rapidly drops at 370 K. The $(\text{Ge}_1\text{Sb}_2\text{Te}_4)_{0.8}(\text{Sn}_1\text{Bi}_2\text{Te}_4)_{0.2}$ alloy shows similar behavior with $\text{Ge}_1\text{Sb}_2\text{Te}_4$ alloy in this regard; however, its transition temperature of 485 K is higher than that of the $\text{Ge}_1\text{Sb}_2\text{Te}_4$ alloy. Figure 2 show TEM micrographs and diffraction patterns of an as-deposited and annealed film before and after the transition temperature in both alloys. Procedures for sample preparation were as follows: 75-nm-thick films were deposited on the SiO-coated TEM grids and then annealed at selective temperatures under an Ar atmosphere. In the case of as-deposited $\text{Ge}_1\text{Sb}_2\text{Te}_4$, shown in Figure 2(a), diffraction halos were clearly observed in conjunction with a mostly featureless bright field image caused by the dominant amorphous matrix. Some crystallites within the amorphous matrix indicate that the crystallization kinetics of this material is relatively fast as compared with other GeSbTe compounds; for instance, $\text{Ge}_2\text{Sb}_2\text{Te}_5$ shows no crystallite in the as-deposited film^[5]. In contrast, the diffraction ring patterns of the as-deposited $(\text{Ge}_1\text{Sb}_2\text{Te}_4)_{0.8}(\text{Sn}_1\text{Bi}_2\text{Te}_4)_{0.2}$ (Figure 2(b)) can be analyzed as having an *fcc* structure, with small grains 20 nm in diameter on average. Figure 2(c) shows the TEM micrograph and the selected area diffraction pattern of the $\text{Ge}_1\text{Sb}_2\text{Te}_4$ film annealed at 200 °C (after transition). The analysis of TEM diffraction pattern clearly shows that a single *fcc* crystalline phase is formed and the bright field TEM image shows that the microstructure for $\text{Ge}_1\text{Sb}_2\text{Te}_4$ film is composed of small grains 10 nm on average. After annealing at 300 °C (after transition) for $(\text{Ge}_1\text{Sb}_2\text{Te}_4)_{0.8}(\text{Sn}_1\text{Bi}_2\text{Te}_4)_{0.2}$, the diffraction pattern appears perpendicular to the surface and [0001] orientation of the film with $a \approx 0.42$ nm and arrows indicate the weak $\{10^{-1}0\}$ patterns of single *hcp* phase (Figure 2(d)). It should be noted that the microstructure evolutions of $\text{Ge}_1\text{Sb}_2\text{Te}_4$ and $(\text{Ge}_1\text{Sb}_2\text{Te}_4)_{0.8}(\text{Sn}_1\text{Bi}_2\text{Te}_4)_{0.2}$ are quite different. The microstructure of the $\text{Ge}_1\text{Sb}_2\text{Te}_4$ single layer contains extremely small grains, while that of $(\text{Ge}_1\text{Sb}_2\text{Te}_4)_{0.8}(\text{Sn}_1\text{Bi}_2\text{Te}_4)_{0.2}$ contains much larger grains. While further study is required, it is tentatively assumed that these differences in microstructure evolution are closely related to the phase transformation modes. It is generally accepted that the crystallization of the GeSbTe material is dominated by nucleation^[6], which results in a small grain size. On the contrary, the phase transformation from *fcc* to *hcp* in the $(\text{Ge}_1\text{Sb}_2\text{Te}_4)_{0.8}(\text{Sn}_1\text{Bi}_2\text{Te}_4)_{0.2}$ alloy material appears to be dominated by a grain growth mode. Furthermore, our results clearly indicate that the sheet resistance drop in $\text{Ge}_1\text{Sb}_2\text{Te}_4$ corresponds to a phase transition, from amorphous to *fcc* crystalline, while the resistance drop in $(\text{Ge}_1\text{Sb}_2\text{Te}_4)_{0.8}(\text{Sn}_1\text{Bi}_2\text{Te}_4)_{0.2}$ is caused by the transition from *fcc* to *hcp* crystalline.

3.3. Kinetics of the phase transformations

Kissinger's method^[7] is useful tool with which to analyze the kinetics of structural transformation. It is well known that one

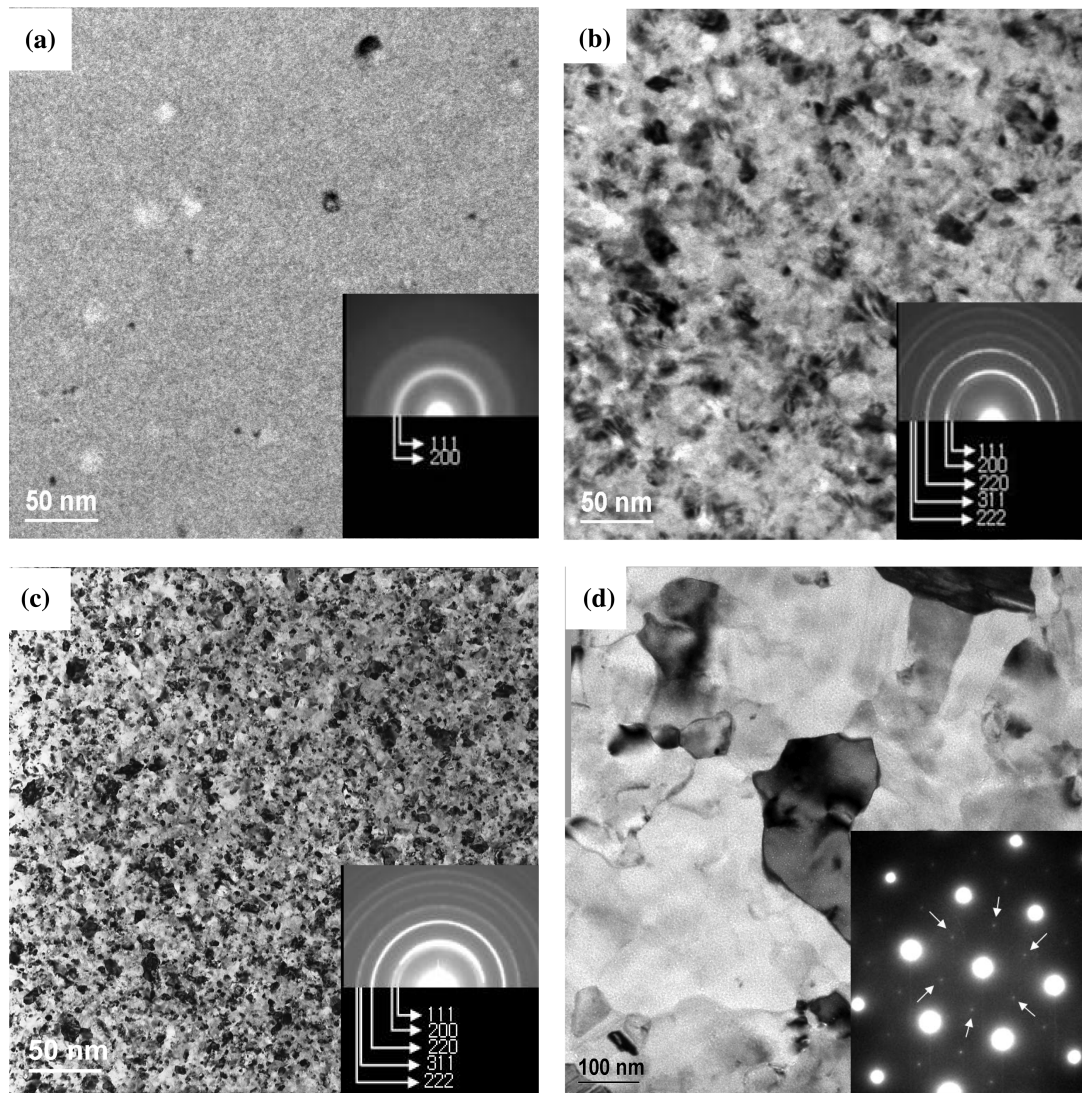


Fig. 2. TEM micrographs and diffraction patterns of two alloys. All samples were prepared on SiO-coated TEM grids.

- (a) $\text{Ge}_1\text{Sb}_2\text{Te}_4$, as-deposited *amorphous* phase
- (b) $(\text{Ge}_1\text{Sb}_2\text{Te}_4)_{0.8}(\text{Sn}_1\text{Bi}_2\text{Te}_4)_{0.2}$, as-deposited *fcc* phase
- (c) $\text{Ge}_1\text{Sb}_2\text{Te}_4$, annealed at 200 °C - 15 minutes, *fcc* phase
- (d) $(\text{Ge}_1\text{Sb}_2\text{Te}_4)_{0.8}(\text{Sn}_1\text{Bi}_2\text{Te}_4)_{0.2}$, annealed at 300 °C - 15 minutes, *hcp* phase

can obtain the overall kinetic activation energy from a Kissinger plot if a given transformation is a thermal activation process. There are several ways to measure the transition temperature for each heating rate in Kissinger equation, including optical measurement, Differential scanning calorimetry (DSC), and electrical measurement. Among these methods, if sample is thinfilm and no optical property changes before and after transition, electrical measurement is very useful. In this study, since no film showed a reflectivity difference between the *fcc* and *hcp* phase, *in-situ* sheet resistance measurement was achieved. To calculate the activation energies of the two alloys, the heating rate was varied from 0.05 ~ 0.275 K/sec. The calculation results are shown in Fig. 3(a) and (b). The transition temperature, T_t , at each heating rate is obtained

by the minimum of the first derivative of sheet resistance (dR_s/dt), and the transformation activation energy, E_a , is determined by the slope k ($k = -E_a/k_b$, k_b : Boltzmann's constant) of the linear fit in the corresponding Kissinger plot. The Kissinger plots of $\text{Ge}_1\text{Sb}_2\text{Te}_4$ and $(\text{Ge}_1\text{Sb}_2\text{Te}_4)_{0.8}(\text{Sn}_1\text{Bi}_2\text{Te}_4)_{0.2}$ are shown in Figure 4(a) and (b). In Figure 4(a), the activation energy of amorphous to *fcc* transformation in $\text{Ge}_1\text{Sb}_2\text{Te}_4$ alloy is shown to be 1.85 ± 0.4 eV. This value agrees well with previous reported values, which were obtained from DSC analysis (1.82 eV) by Noboru Yamada *et al.*^[8]. For the $(\text{Ge}_1\text{Sb}_2\text{Te}_4)_{0.8}(\text{Sn}_1\text{Bi}_2\text{Te}_4)_{0.2}$ alloy, the transformation activation energy from *fcc* to *hcp* is 2.98 ± 1.6 eV, and this value is smaller than that of the $\text{Ge}_2\text{Sb}_2\text{Te}_5$ (3.64 ± 0.19 eV for *fcc* to *hcp*, 2.24 ± 0.11 eV for *amorphous* to *fcc*), which was obtained from sheet resistance

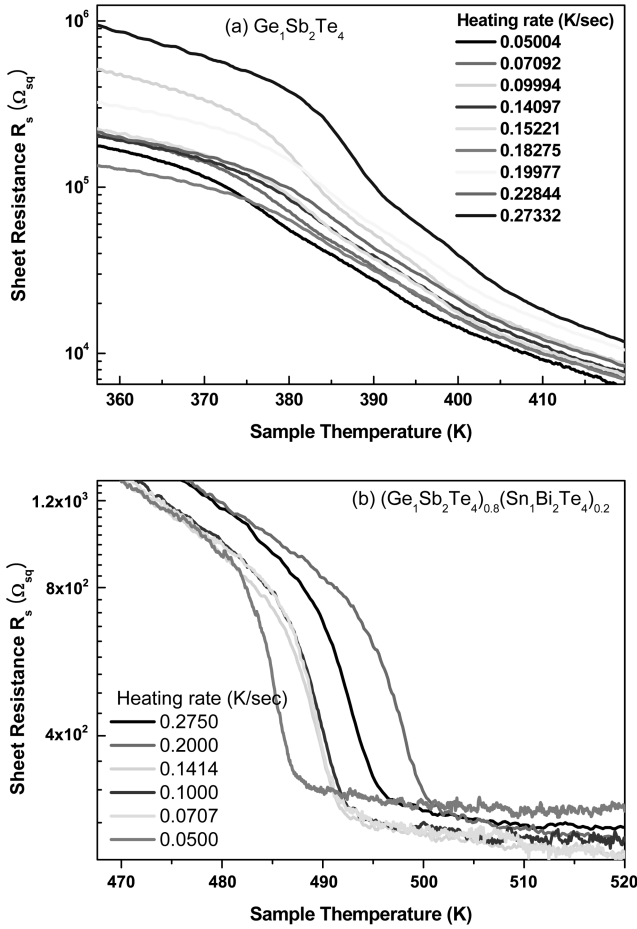


Fig. 3. Temperature dependence of the sheet resistance R_s of (a) $\text{Ge}_1\text{Sb}_2\text{Te}_4$ and (b) $(\text{Ge}_1\text{Sb}_2\text{Te}_4)_{0.8}(\text{Sn}_1\text{Bi}_2\text{Te}_4)_{0.2}$ films, as measured with different heating rates.

analysis by I. Friedrich *et al.*^[4]. From these results, we concluded that the transformation activation energy from *fcc* to *hcp* in $(\text{Ge}_1\text{Sb}_2\text{Te}_4)_{0.8}(\text{Sn}_1\text{Bi}_2\text{Te}_4)_{0.2}$ is larger than that of the *amorphous* to *fcc* phase in $\text{Ge}_1\text{Sb}_2\text{Te}_4$, but smaller than that of the *fcc* to *hcp* transformation in $\text{Ge}_2\text{Sb}_2\text{Te}_5$. It is believed that these are the reasons why rapid *fcc* to *hcp* transition is possible in phase change memory with $(\text{Ge}_1\text{Sb}_2\text{Te}_4)_{0.8}(\text{Sn}_1\text{Bi}_2\text{Te}_4)_{0.2}$, and it is expected that this type of memory device will show high retention characteristics, judging from its high transition activation energy. According to our previous study^[9], such accelerated phase transformation kinetics in this new alloy added to $\text{Sn}_1\text{Bi}_2\text{Te}_4$ is to the result of the reduced strengths of various inter-atomic bonds in this alloy.

4. SUMMARY

The phase transformation kinetics of a $(\text{Ge}_1\text{Sb}_2\text{Te}_4)_{0.8}(\text{Sn}_1\text{Bi}_2\text{Te}_4)_{0.2}$ alloy mixture were studied using *in-situ* temperature-dependent sheet resistance measurement and TEM analysis. An as-deposited crystalline *fcc* phase is transformed

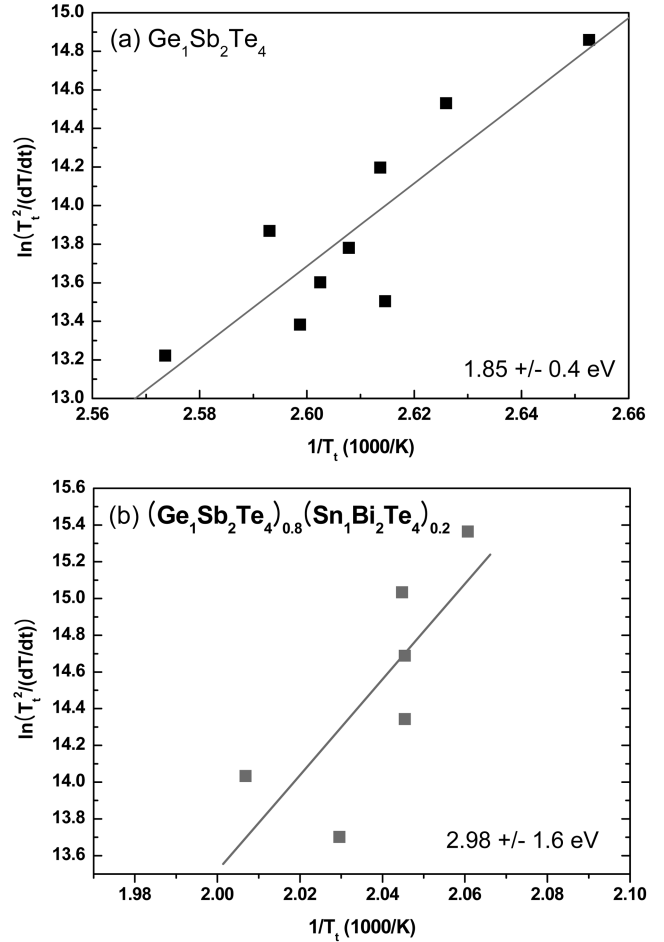


Fig. 4. Kissinger plots of (a) $\text{Ge}_1\text{Sb}_2\text{Te}_4$ and (b) $(\text{Ge}_1\text{Sb}_2\text{Te}_4)_{0.8}(\text{Sn}_1\text{Bi}_2\text{Te}_4)_{0.2}$ films. Transformation activation energy was determined from the slope, k , of the Kissinger plot. Obtained activation energies were 1.85 ± 0.4 eV for (a) and 2.98 ± 1.6 eV for (b).

at 485 K to a *hcp* phase in $(\text{Ge}_1\text{Sb}_2\text{Te}_4)_{0.8}(\text{Sn}_1\text{Bi}_2\text{Te}_4)_{0.2}$ alloy; this transformation temperature is in contrast with that of $\text{Ge}_1\text{Sb}_2\text{Te}_4$ film, which transforms from *amorphous* to *fcc* crystalline phase at 370 K. The activation energies of both phase transformations were determined using Kissinger's method. The obtained activation energy was 1.85 eV for *amorphous* to *fcc* and 2.98 eV for *fcc* to *hcp*. These values correspond well to the previously published data. In addition, these results explain why rapid *fcc* to *hcp* transition is possible in phase change memory using $(\text{Ge}_1\text{Sb}_2\text{Te}_4)_{0.8}(\text{Sn}_1\text{Bi}_2\text{Te}_4)_{0.2}$, and it is expected that this type of memory device will show high retention characteristics.

ACKNOWLEDGEMENT

This work was supported in part by the National Research Program for 0.1 Terabit Non-volatile Memory Development sponsored by the Korea Ministry of Science and Technology.

REFERENCES

1. Ron Neale, *Electronic Engineering*, April, 67 (2001).
2. D.-H. Ahn, D.-H. Kang, B.-K. Cheong, H.-S. Kwon, M.-H. Kwon, T.-Y. Lee, J.-H. Jeong, T. S. Lee, I. H. Kim, and K.-B. Kim, *Electron Device Lett.* May, 286 (2005).
3. L. J. van der Pauw, *Philips Res. Rep.* **13**, 1 (1958).
4. I. Friedrich, V. Weidenhof, W. Njoroge, P. Franz, and M. Wuttig, *J. Appl. Phys.* **87**, 4130 (2000).
5. Jon Maimon, Ed Spall, Robert Quinn, and Steven Schnur, *IEEE Aero Space Conference*, p. 2289 (2001).
6. M. Terao, S. J. Hudgens, S. R. Ovshinsky, M. Mansuripur, and M. Wuttig, "Phase Change Data Storage", *Tutorial hand book of MRS fall* (2004).
7. H. E Kissinger, *Anal. Chem.* **29**, 1702 (1957).
8. N. Yamada, E. Ohno, K. Nishiuchi, N. Akahira, and M. Takao, *J. Appl. Phys.* **69**, 2849 (1991).
9. T.-Y. Lee, K.-B. Kim, B.-K. Cheong, T.-S. Lee, S. J. Park, K. S. Lee, W. M. Kim, and S. G. Kim, *Appl. Phys. Lett.* **80**, 3313 (2002).